Hydrometeorological Conditions Preceding Extreme Streamflow for the Charles and Mystic River Basins of Eastern Massachusetts

LAURIE AGEL AND MATHEW BARLOW

University of Massachusetts Lowell, Lowell, Massachusetts

MATHIAS J. COLLINS

National Marine Fisheries Service, National Oceanic and Atmospheric Administration, Gloucester, Massachusetts

ELLEN DOUGLAS AND PAUL KIRSHEN

School for the Environment, University of Massachusetts Boston, Boston, Massachusetts

(Manuscript received 25 January 2019, in final form 23 May 2019)

ABSTRACT

Hydrometeorological links to high streamflow events (HSFEs), 1950–2014, for the Mystic and Charles watersheds in the Metro Boston region of Massachusetts are examined. HSFEs are defined as one or more continuous days of streamflow above the mean annual maxima for a selected gauge in each basin. There are notable differences in the HSFEs for these two basins. HSFEs last from 1 to 3 days in the Mystic basin, while HSFEs for the Charles can last from 3 to 9 days. The majority of Mystic HSFEs are immediately preceded by extreme precipitation (occurring within 24 h), while only half of those for the Charles are preceded by extreme precipitation (in this case occurring 2–5 days earlier). While extreme precipitation events are often linked to HSFEs, other factors are often necessary in generating high streamflow, particularly for the Charles, as more than 50% of HSFEs occur at times when streamflow, soil moisture, and total precipitation are statistically above average for a period of at least 2 weeks before the HSFE. Approximately 52% and 80% of HSFEs occur from February to June for the Mystic and Charles, respectively, and these HSFEs are frequently linked to the passage of strong coastal lows, which produce extreme precipitation in the form of both rain and snow. For these coastal lows, Mystic HSFEs are linked to a strong moisture feed along the Massachusetts coastline and intense precipitation, while Charles HSFEs are linked to strong cyclones located off the Mid-Atlantic and longer-duration precipitation.

1. Introduction

The New England region of the U.S. Northeast is vulnerable to multiple flood regimes, including coastal floods, river floods, urban drainage floods, and flash floods. In New England, flash floods tend to occur mostly in small, high-relief, and/or urbanized basins. The human cost of floods is twofold: economic loss through the damage of property, infrastructure, and agriculture and the loss of life. Two of the most costly flood events in recent Northeast history include a long-duration extratropical cyclone in May 2006, which caused over $70 million in damages in Massachusetts due to river flooding (Federal Emergency Management Agency 2006), and Hurricane Irene in 2011, which caused nearly $7 billion in flood damages in Vermont (Melillo et al. 2014). Most flood fatalities in New England occur during the summer months, and the majority of these fatalities are associated with flash floods (Ashley and Ashley 2008).

A variety of factors can affect river, flash, and urban drainage floods, with precipitation being the most predominant. Short, intense rain events can cause urban drainage floods and/or flash floods in small and/or urbanized basins, while moderate-duration, high-intensity events, and long-duration events of varying intensities

Denotes content that is immediately available upon publication as open access.

Supplemental information related to this paper is available at the Journals Online website: https://doi.org/10.1175/JHM-D-19-0017.s1.

Corresponding author: Laurie Agel, laurie_agel1@uml.edu

DOI: 10.1175/JHM-D-19-0017.1

can cause river floods. In the Northeast, heavy precipitation is often associated with the occurrence of extratropical cyclones and tropical cyclones (Agel et al. 2019; Hawcroft et al. 2012; Pfahl and Wernli 2012). It is important to note that extreme precipitation does not always result in flooding (Ivancic and Shaw 2015). Other factors often determine basin response to extreme precipitation events, including basin size and topography, infiltration capacity, basin storage (e.g., lakes or wetlands), antecedent conditions such as saturated or frozen soil, evapotranspiration, snow cover, and snowmelt. Further, anthropogenic factors such as land use (e.g., urbanization), dams, or other water diversions can affect runoff magnitude and timing and lead to, exacerbate, or moderate flood events.

Several studies have examined the linkage between New England river floods and precipitation. Collins et al. (2014), using over 50 years of data at 10 individual gauges, found that precipitation associated with extratropical cyclones originating from three source regions (Great Lakes storms, Ohio Valley storms, and ''coastal lows'') produce the majority of annual floods in New England. The majority of the annual maxima (approximately 60%) occur from late winter to early spring. The dominant mechanism for annual floods was found to be precipitation (approximately 70%), often in conjunction with high antecedent soil moisture, and precipitation combined with snowmelt. Towey et al. (2018) found that 43% of the top-100 streamflow events for the Ashokan Reservoir of New York were also associated with top-100 basin-scale 1-day precipitation and multiday precipitation events, most of which were associated with passing extratropical cyclones. This result is similar to that found by Ivancic and Shaw (2015), in which 99th percentile precipitation resulted in 99th percentile river discharge 36% of the time. For the Towey et al. (2018) study, the majority of top-100 streamflow events occurred from December to April, although the highest precipitation events occurred from June to November. Many of the top-100 streamflow events occurred in conjunction with anomalously high near-surface warming and humidity. Top-100 streamflow events without concurrent heavy precipitation events occurred primarily in the cool season, leading the researchers to speculate that high-streamflow events (HSFEs) in this season were likely associated with snowmelt due to anomalous warmth. Graybeal and Leathers (2006) also found snowmelt to be associated with enhanced flood frequency in the Appalachian Mountains of the Northeast. However, other researchers have noted that high antecedent soil moisture associated with seasonally low evapotranspiration is often at least as important as snowmelt for spring flood occurrences in New England and New York (Collins et al. 2014; Collins 2019).

The link between extreme precipitation and flooding is fundamental to understanding how flood frequency and intensity may change in a warming climate. Extreme daily precipitation has increased significantly in the Northeast (Kunkel et al. 2013), with the period 1996–2014 experiencing 53% higher extreme precipitation than 1901–95 (Huang et al. 2017). Because most extreme precipitation occurs during the warm months and autumn in the Northeast (Agel et al. 2015), but the majority of floods occurs from late winter to early spring, trends in floods tend to be weaker and more difficult to assess (Frei et al. 2015; Ivancic and Shaw 2015). Nevertheless, there are positive trends in flood magnitude and frequency in the Northeast (Armstrong et al. 2012, 2014; Collins 2009; Peterson et al. 2012; Slater and Villarini 2016).

In this study we look at two adjacent river basins that drain into Boston Harbor (Fig. 1), with very different storage capacities and responses to precipitation. The Charles River basin and its associated watershed, located west of Boston, comprises a collection of streams, wetlands, and ponds feeding into the nearly 130-km-long, meandering Charles River, with a total drainage area of 798 km^2. Along its length, the river supports a population of close to 900 000 people and flows through 23 cities or towns, making the watershed one of the most densely populated in New England (Charles River Watershed Association; https://www.crwa.org/charles-river-watershed). The Mystic River Watershed northwest of Boston has a drainage area of approximately 197 km^2 and flows through over 20 communities (https://mysticriver.org/the-watershed). For both river basins, streamflow is impacted by diversions, dams and reservoirs, and heavy urbanization, particularly near their outlets at Boston Harbor. Because of the vulnerability of the towns and communities within these basins to floods, it is important to understand the meteorological conditions and other precursors that can lead to flooding in this region.

For these two basins we examine multiple factors associated with floods, concentrating on precipitation, and tie that to meteorological causes. In particular we investigate the links between HSFEs and extreme precipitation, and examine the dynamical meteorological mechanisms underlying the occurrence of extreme precipitation. In addition, we examine several surface hydrological factors associated with meteorological influences, such as soil moisture, soil surface temperature, snow cover, and snowmelt. Finally, we investigate the differences in the two basins' responses to these factors—what conditions cause a flood in one

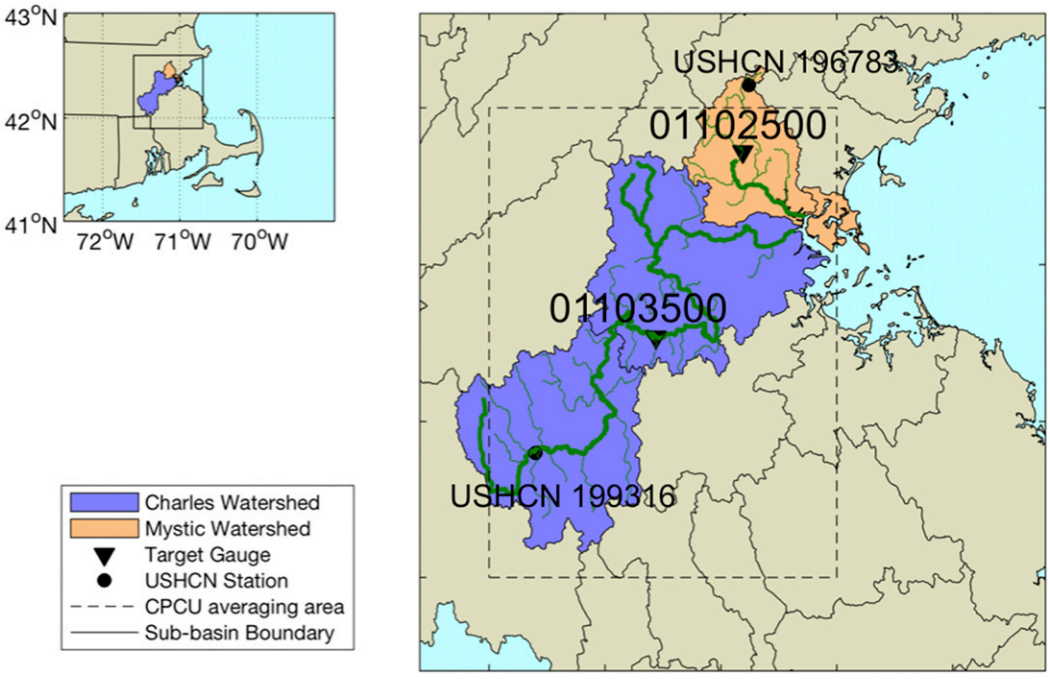

FIG. 1. Locations of the Mystic (orange shading) and Charles (blue shading) basins in eastern Massachusetts and USGS surface water gauges with long-running daily data (01102500 at Winchester, MA, and 01103500 at Dover, MA; black triangles) chosen to represent each basin, respectively. Closest upstream USHCN precipitation observation station locations for each gauge are also shown (196783 at Reading, MA, and 199316 at West Medway, MA; black dots).

river and not the other, and can we use that information to better predict when and where flooding occurs?

The remainder of this study is organized as follows. In section 2, the data and methods used in the study are presented. In section 3, the characteristics of HSFEs are detailed, followed by an examination of the meteorological links and antecedent conditions associated with the HSFEs. In section 4, key findings are summarized and discussed.

2. Data and methods

a. Streamflow

The United States Geological Survey (USGS) provides daily data for stream gauges through the USGS Surface-Water Daily Data for the Nation (https://waterdata.usgs.gov/nwis/sw). For this study, we examine mean daily streamflow ($m^3 s^{-1}$), 1950–2014, for the Charles River gauge at Dover, MA (USGS 01103500), and the Aberjona River gauge at Winchester, MA (USGS 01102500), in the Charles and Mystic basins, respectively. The mean daily value is the average over ninety-six 15-min instantaneous values. Gauge locations are marked by the large black triangles in Fig. 1. These gauges were selected for their long-term data availability, completeness (no missing days), and position at the center of their respective river basins. Although both gauges are located upstream of the more significant water management measures that protect the urbanized and high-population communities at the mouths of their respective rivers near Boston Harbor, both are still situated in moderately to highly developed subwatersheds. As such, streamflow—including floods—for both basins is affected to unknown degrees by regulation and/or diversions (USGS peak flow qualification code 5) for their entire records. However, we believe these conditions do not substantially affect our results because they have been relatively consistent for our period of analyses.

High-streamflow days are defined as those with streamflow above the mean annual flood (MAF) value for each gauge, based on annual maximum average daily flows, 1950–2014. Flow levels exceeding the MAF tend to be higher than ''bankfull flows,'' which have annual recurrence intervals of around 1.5 years (Wolman and Miller 1960), and generally represent true overbank conditions. This threshold corresponds to $11.3\,m^3 s^{-1}$ for the Mystic gauge and $40.6\,m^3 s^{-1}$ for the Charles gauge. Consecutive days of above-threshold streamflow are grouped into HSFEs, with the peak streamflow date serving to identify each event. This results in

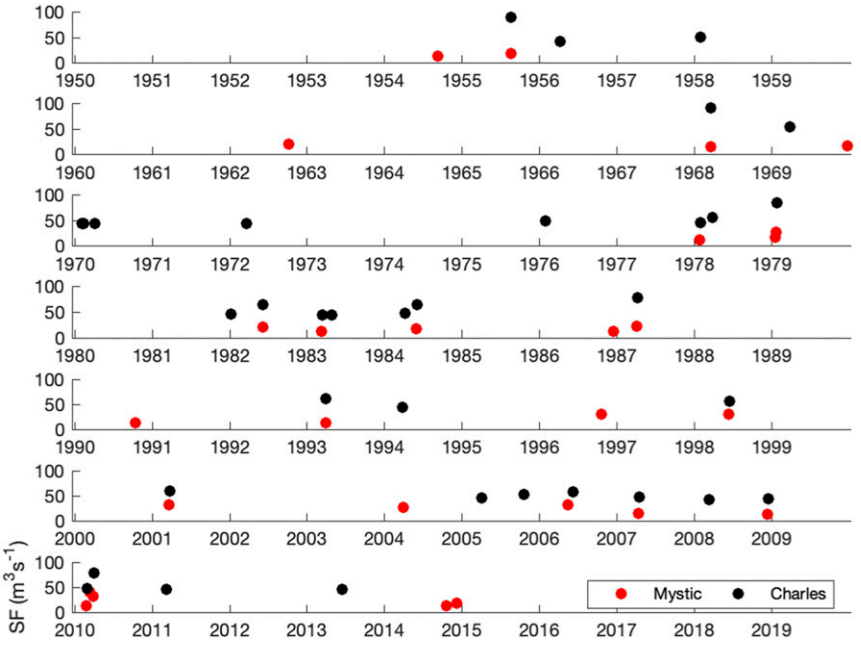

FIG. 2. HSFE peak date and corresponding streamflow ($m^3 s^{-1}$) for the Mystic (red dots) and Charles (black dots), 1950–2014.

34 HSFEs for the Charles basin and 27 HSFEs for the Mystic basin, with the duration of each HSFE defined as the length of time in days that the streamflow remains at or above the threshold value. The timeline of HSFE occurrences is shown in Fig. 2. Notably, HSFEs do not always occur in the Charles basin when they occur in the Mystic basin, and vice versa.

Streamflow anomalies at each gauge are found by subtracting long-term daily mean streamflow from each daily streamflow value (e.g., the 1 January long-term daily mean is subtracted from each 1 January value). Long-term daily mean streamflow is calculated by taking the 65-yr mean of each calendar day (e.g., the mean of all 1 January values), and smoothing the resulting 366-day time series with a 14-day running mean.

The Richards–Baker flashiness index (Baker et al. 2004), which relies on average daily flow data, is computed for each basin. The index is a number from 0 (low flashiness) to 1 (high flashiness). Flashier streams are characterized by more frequent and rapid short-term changes in streamflow (Baker et al. 2004). For water year 2016, the Charles basin has a flashiness index of 0.08, while the Mystic basin has an index of 0.28. The lower value for the Charles is reflective of both the larger basin size and larger storage capacity in terms of upstream lakes, ponds, and wetlands. Both of these indices are rather low for urban basins in general, but are consistent with values at other gauges in eastern Massachusetts, due to the relatively low relief of the area, and upstream water storage in the form of ponds, lakes, and wetlands. Related to flashiness is the watershed response time (WRT) to precipitation events, which we estimate to be 0–1 day for the Mystic gauge and 2–5 days for the Charles gauge. Our estimates of WRT roughly correspond to the centroid lag-to-peak measure—the time that elapses from the center-of-volume of the rain event to the peak streamflow (Dingman 2002). Table 1 summarizes the characteristics of the two gauges, including MAF threshold, flashiness index, number of HSFEs, and mean duration of HSFEs.

b. *Precipitation*

Daily gridded precipitation from the National Oceanic and Atmospheric Administration (NOAA) Climate Prediction Center (CPC) 0.25° × 0.25° Daily U.S. Unified Precipitation (CPCU; Chen et al. 2008), available at https://www.esrl.noaa.gov/psd/data/gridded/data.unified.daily.conus.html, is used to create areal precipitation means for each day, 1950–2014, for the 0.5° × 0.5° box outlined by the dashed line in Fig. 1. The CPCU dataset was chosen for its continual coverage of the study period, and its close correlation to station data available within the basins. As a complement to the gridded data, we also consider daily station observations from the United States Historical Climatology Network (USHCN; Easterling et al. 1999)

TABLE 1. Summary of gauge data for the Mystic and Charles basins, 1950–2014, including the water response time (WRT), flash index, mean annual flood (MAF) threshold and number of days with streamflow over that value, number of high streamflow events (HFSEs), and average duration of the HSFEs.

Basin	USGS gauge	WRT	Baker flash index	MAF ($m^3 s^{-1}$)	Days over MAF	No. of HSFEs	Mean HSFE duration (days)
Mystic	01102500	0–1	0.28	11.3	233	27	2.0
Charles	01103500	2–5	0.08	40.6	239	34	7.0

West Medway station (USHCN 199316), near the head of the Charles River, and the Reading station (USHCN 196783), near the headwaters of the Mystic River (Fig. 1). USHCN precipitation data are available from https://cdiac.ess-dive.lbl.gov/ftp/ushcn_daily. The West Medway station includes data from 1957 to 2005, with 0.3% days missing in that range, while the Reading station includes data from 1960 to 2014, with 0.01% days missing in that range. Long-term daily means of precipitation are calculated as for streamflow. Although neither USHCN station has complete records for time period studied, they provide an important secondary data source to confirm links between heavy streamflow and gridded precipitation.

c. *Reanalysis data*

The Modern Era Retrospective Reanalysis for Research and Application (MERRA-2; Gelaro et al. 2017) from the National Aeronautics and Space Administration (NASA), available at https://disc.gsfc.nasa.gov/datasets?keywords=MERRA-2, is used to establish the meteorological conditions associated with the HSFEs. The fields examined include upper-level circulation (tropopause pressure and 500-hPa geopotential height), mean sea level pressure (MSLP), and integrated

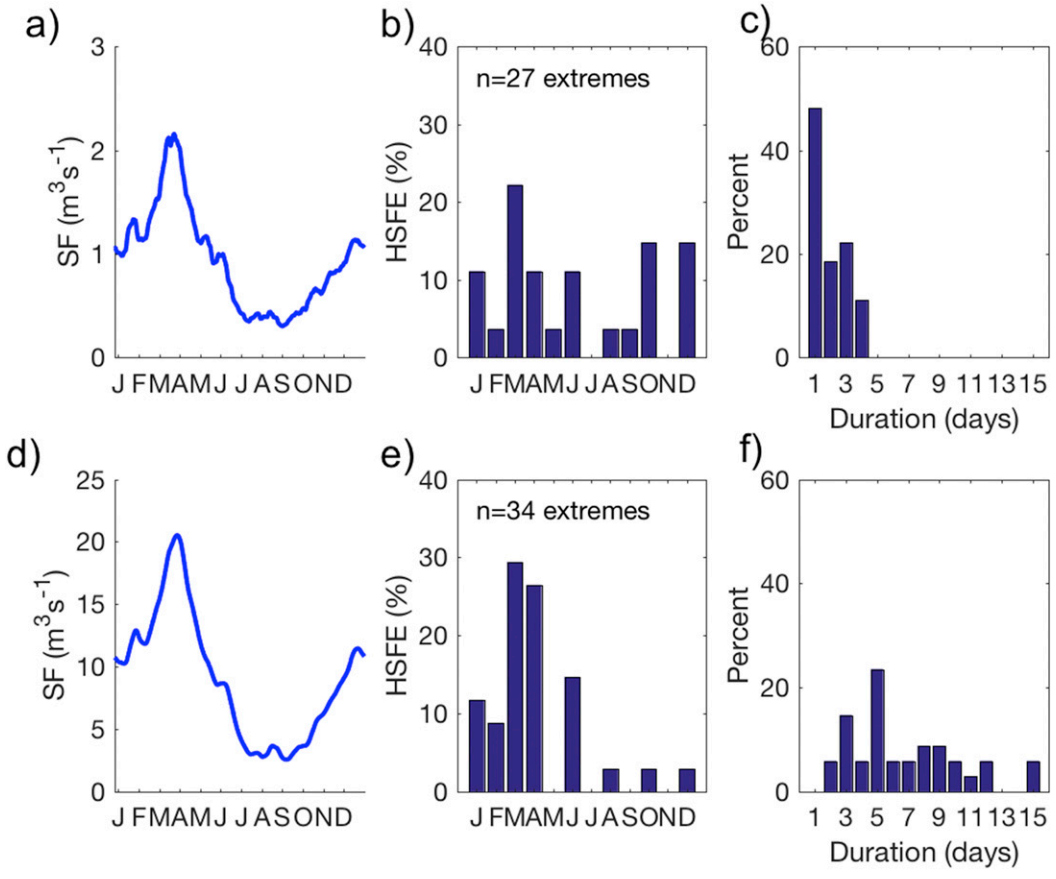

FIG. 3. Mystic gauge (a) long-term daily mean of streamflow ($m^3 s^{-1}$), (b) seasonality of HSFEs (percent of events by month), and (c) duration of HSFEs (percent of total events for various lengths in days), 1950–2014. (d)–(f) As in (a)–(c), but for the Charles gauge.

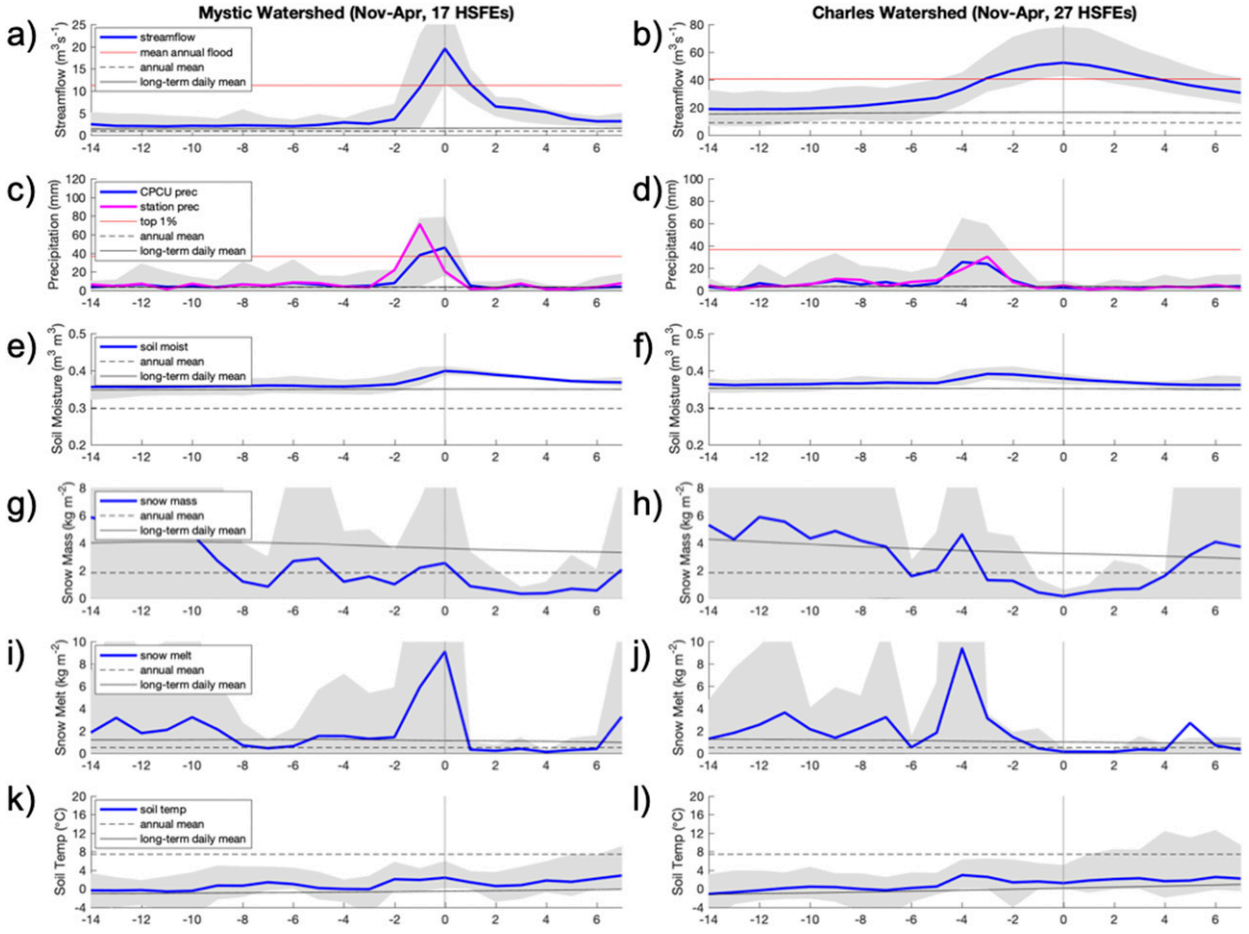

FIG. 4. Composite (a),(b) streamflow ($m^3 s^{-1}$), (c),(d) precipitation (mm day^{-1}), (e),(f) soil moisture ($m^3 m^{-3}$), (g),(h) snow mass ($kg m^{-2}$), (i),(j) snowmelt ($kg m^{-2}$), and (k),(l) soil temperature (°C) for the 22-day periods surrounding the November–April HSFEs, 1950–2014, at the (left) Mystic and (right) Charles watershed gauges, beginning 14 days before and ending 7 days after the peak day of each HSFE. Day "0" (vertical gray line) marks the peak of the HSFEs. Panels (e)–(l) relate only to HSFEs that occur after 1979. For each composite trace, the long-term daily mean (22-day traces of long-term daily means associated with each HSFE, composited) is shown as a black line, while the annual mean is shown as a dashed black line. For streamflow, the horizontal red line marks the threshold used to define HSFEs; and for precipitation, the horizontal red line marks the top 1% threshold used to define extreme precipitation. Precipitation is the areal average of four CPCU grid boxes encompassing the watersheds, while soil moisture, snow mass, snowmelt, and soil temperature are the areal average of two MERRA-Land grid boxes encompassing the watersheds. The gray shading surrounding the blue composite lines represents the 10%–90% values for the individual HSFEs that make up the composite.

water vapor transport (IVT). In addition, MERRA-Land (Reichle et al. 2011) is used to examine soil wetness, soil temperature, snowmelt, and snow cover (snow mass). MERRA-Land provides improved land surface hydrological fields, based on adjustments to global precipitation forcing estimates and rainfall interception model parameters. MERRA-2 and MERRA-Land are available from 1980 to present. Comparisons of HSFEs to MERRA-2 hydrological and meteorological fields are limited to those events that occur from 1980 to 2014 (19 events for the Mystic, and 21 events for the Charles). Long-term daily means of the MERRA-2 and MERRA-Land fields are calculated as for streamflow, and where used, anomaly fields are calculated by subtracting the long-term daily mean from each daily value.

d. Time series

For each HSFE, time series of various data (streamflow, precipitation, snow cover, etc.) are constructed from 14 days prior to the HSFE peak day extending to 7 days after the HSFE peak day, resulting in 22-day time series. Similarly, time series of long-term daily means of various data for the HSFEs are constructed from 14 days prior to the HSFE peak calendar day (e.g., 18 January for a 1 February 1955 peak) extending to 7 days after the peak calendar day (e.g., 8 February). Composites of time

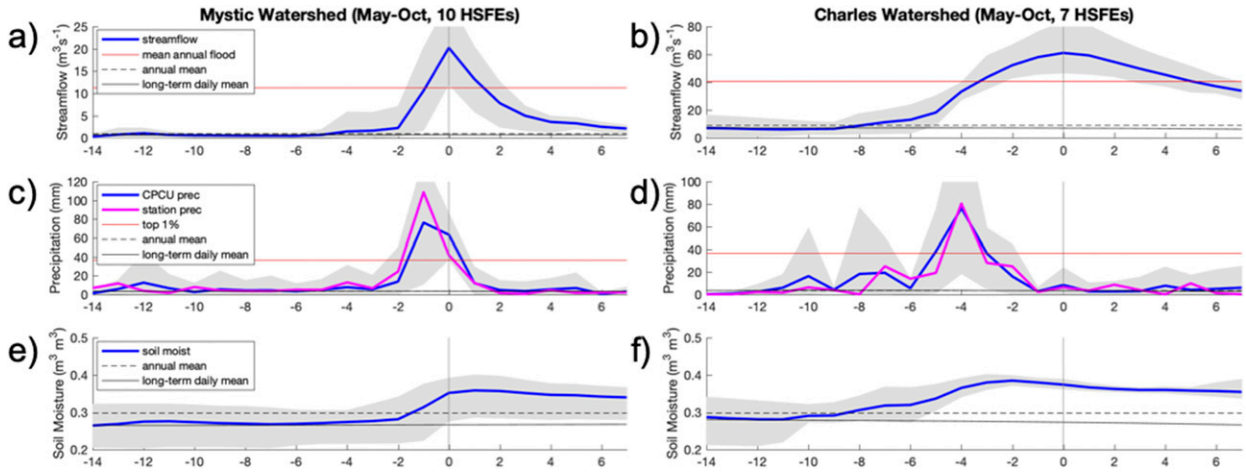

FIG. 5. As in Fig. 4, but for the May–October HSFEs.

series are created for each variable by taking the mean of each day in the set of 22-day time series for the 34 Charles HSFEs and the 27 Mystic HSFEs.

e. *Significance*

Unless otherwise noted, statistical significance is calculated by Monte Carlo resampling, in which a given observed value, for example, antecedent snowmelt, is recalculated at least 1000 times using random samples of the data with the same sample size and seasonal frequency as the original observed value. The top and bottom 2.5% of the random test values are used to establish significance at the 0.05 level.

3. Results

a. *Streamflow and HSFEs*

The long-term daily means of streamflow for the two gauges are shown in Figs. 3a and 3d. These display a typical Northeast U.S. annual cycle, in which streamflow is highest in late winter and early spring and lowest from July to September. The seasonal frequency of the HSFEs closely follows the streamflow seasonal cycle (Figs. 3b,e). However, HSFEs can and do occur at times when the long-term daily streamflow is low (e.g., both basins feature a HSFE that occurs in August). A manual comparison of the HSFE dates and tropical systems from HURDAT2 (Landsea and Franklin 2013) shows that many warm-season HSFEs are related to tropical precipitation (4 out of 6 of the August–October HSFEs for the Mystic are related to tropical systems; while for the Charles, 1 of the 2 August–October HSFEs is related to a tropical system).

HSFE durations vary as shown in Figs. 3c and 3f. For the Mystic, 48.1% of HSFEs last a single day, while another 40.7% persist for 2–3 days. Duration of HSFEs is typically much longer at the Charles gauge, with no HSFEs lasting a single day and 73.5% of events persisting from 3 to 9 days. These values likely reflect the comparative "flashiness" of each basin.

b. *Relationship of HSFEs to precipitation*

In Figs. 4a–d and 5a–d, composite streamflow and daily precipitation for cold season (November–April) and warm season (May–October) HSFEs, respectively, are shown for the 14 days preceding and the 7 days following HSFEs at the two gauges. Preceding rain occurs 0–1 day before HSFEs for the Mystic gauge, and 2–5 days before HSFEs for the Charles gauge, consistent with the WRTs of the two basins. The duration of the precipitation events tends to be longer for events preceding Charles HSFEs, and shorter for those preceding Mystic HSFEs, particularly for the warm season events. For individual events (not shown), this peak in precipitation generally lasts 1–2 days for Mystic events. For the Charles, however, the precipitation profile preceding the HSFEs can be more complex, with multiple peaks in precipitation, often lasting 2–3 days each. The composite smooths these individual profiles into a single, long-duration event. Notably, the composited precipitation is often extreme or nearly extreme preceding the HSFEs, particularly for the Mystic, and for the Charles during the warm season.

Because extreme precipitation is often linked to HSFEs, we examine how often extreme precipitation events are followed by HSFEs, and conversely, how often HSFEs are preceded by extreme precipitation. From Figs. 6a and 6c, approximately 90% of the Mystic HSFEs are preceded by extreme precipitation, but less than 30% of extreme precipitation events are followed

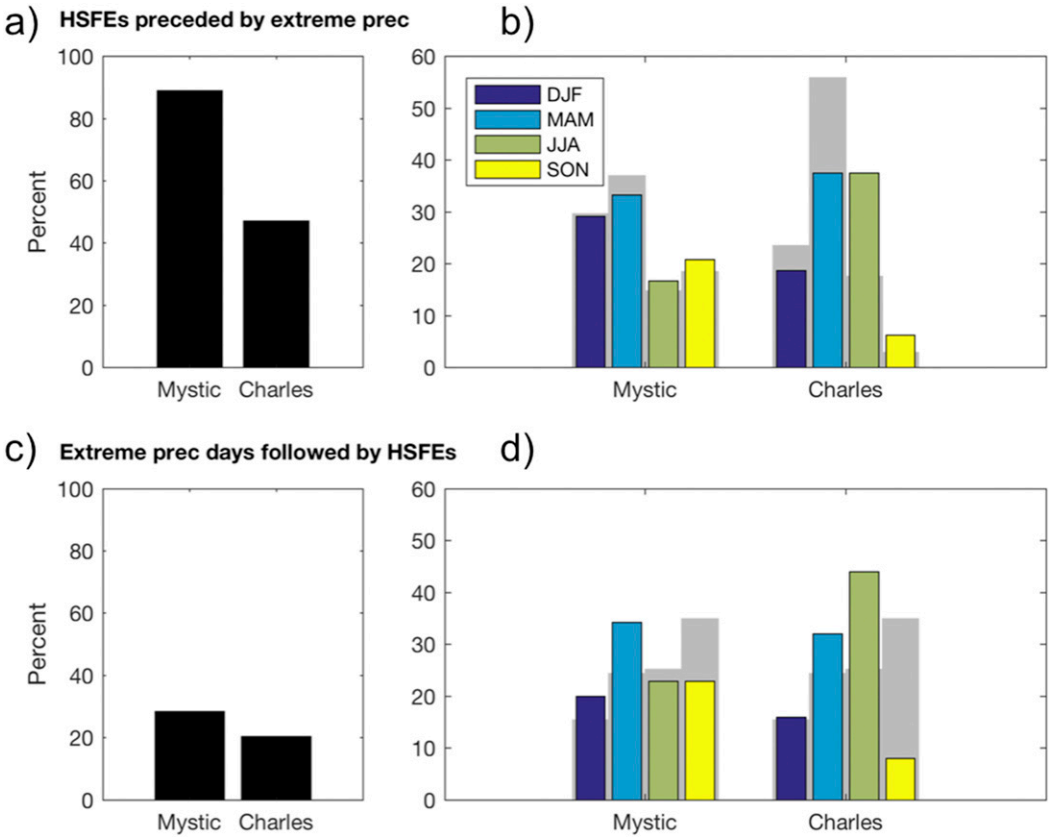

FIG. 6. (a) The percent of HSFE peak streamflow days for the Mystic and Charles that are preceded within 10 days by CPCU top 1% precipitation days and (b) the seasonal percent of the corresponding total bar in (a), with the gray bars showing the seasonal frequency of all HSFEs for each basin (not just those preceded by top 1% days). Conversely, (c),(d) the percent of top 1% CPCU precipitation days that are followed within 10 days by HSFE peak streamflow days, where the gray shading in (d) represents the seasonal frequency of all top 1% precipitation days (not just those followed by HSFEs). CPCU precipitation is based on a mean of four grid boxes surrounding the watersheds.

by HSFEs; while for the Charles basin, nearly 45% of HSFEs are preceded by extreme precipitation, but only 20% of extreme precipitation events are followed by HSFEs, indicating that both basins often require additional factors beyond extreme precipitation to result in HSFEs (a topic explored more in the following sections). These results also reflect the comparatively lower flashiness of the Charles basin—the basin has more storage capacity than that of the Mystic, among other differences such as basin size, that affect response to rainfall events. In contrast, the relatively flashier Mystic basin is linked more directly to precipitation input than to other factors such as storage.

The percent of HSFEs preceded by extreme precipitation is separated into seasonal bins in Fig. 6b (with the gray shading indicating the seasonal separation of all HSFEs for each basin); and the percent of extreme precipitation days followed by HSFEs is separated into seasonal bins in Fig. 6d (with the gray shading indicating the seasonality of all extreme precipitation days). The seasonal breakdown indicates, for both the Mystic and Charles basins, that the need for additional factors or antecedent conditions is most pronounced during MAM and less pronounced for the Charles basin during JJA.

c. *Relationship of HSFEs to soil moisture*

Composite soil moisture increases from slightly above the cold season long-term daily mean (Figs. 4e,f) nearly 10 days before peak streamflow to well above the long-term daily mean during preceding rain events. For warm season events, soil moisture is near the long-term daily mean in the days leading up to the preceding precipitation event (Figs. 5e,f). This may indicate that unusually wet periods precede HSFEs (further explored in section 3f). Additionally, the long-term soil moisture daily mean during cold season HSFEs is higher than the annual mean soil moisture, indicating that HSFEs often occur at times when soil moisture is already seasonally

TABLE 2. Composite standardized anomalies of antecedent indices of streamflow (SF) and CPCU areal precipitation (1950–2014), and MERRA-Land soil moisture, snow mass, snowmelt, and surface soil temperature (1980–2014) for the Mystic and Charles basins, separated into cold-season and warm-season means. Indices are in bold if significant at the 0.05 level.

Basin	Period	No. of HSFEs[a]	SF	CPCU precipitation	Soil moisture	Snow mass	Snowmelt	Soil temperature
Mystic	Nov–Apr	17 (12)	**1.32**	**0.94**	0.32	0.23	0.75	0.22
Mystic	May–Oct	10 (7)	0.16	**0.80**	−0.34	—	—	0.02
Charles	Nov–Apr	27 (15)	**0.69**	**0.75**	**0.40**	**0.81**	**1.59**	−0.05
Charles	May–Oct	7 (6)	0.23	**2.15**	0.23	—	—	0.40

[a] The number of HSFEs used in the composites for SF/CPCU (MERRA-Land variables).

heightened. The soil moisture composite time series closely match the precipitation composite time series preceding these events, indicating that precipitation is an important factor contributing to increased soil moisture in these basins preceding HSFEs.

d. Relationship of cold season HSFEs to snow mass and snowmelt

For cold season HSFEs, snow mass (Figs. 4g,h) tends to decrease just before the preceding precipitation event, increase sharply with the precipitation event, and then decrease again during and just after the event. Relatedly, snowmelt increases from levels near the long-term daily mean in the days preceding HSFEs, and then returns to levels below the long-term daily mean in the days after HSFEs (Figs. 4i,j). This implies that snowmelt (when snow cover exists) plays a large role in contributing to increases in soil moisture before HSFEs. To measure this, we examine snowmelt in a 7-day window preceding all HSFEs that occur December–April 1980–2014 (12 HSFEs for the Mystic, 15 HSFEs for the Charles). The 7-day window is adjusted to end before the WRT for each gauge (0–1 day for the Mystic and 2–5 days for the Charles), in order to capture potential contributions from snowmelt to soil moisture outside of the main precipitation event that often precedes HSFEs. Within this window, 92.3% (100%) of the examined Mystic (Charles) HSFEs feature measurable snowmelt on at least 3 days.

e. Relationship of cold season HSFEs to soil temp

From Figs. 4k and 4l, soil temperature during the cold season tends to be higher than the long-term daily mean preceding and during HSFEs, but well below the annual mean. Since the majority of HSFEs occur from December to June, the lower-than-annual values are expected. However, the fact that soil temperature is higher than the long-term daily mean and well above freezing suggests that frozen earth is not a major factor contributing to flooding within these basins. It does not appear that snow cover plays a significant role in the above-freezing soil temperature for these events, as the soil temperature increases with decreasing snow cover. In addition, the composited long-term daily mean tends to increase over the 22 days, perhaps reflecting the increasing solar radiation that occurs in spring when most of the HSFEs occur, particularly for the Charles. The slight warming of soil temperature during the preceding precipitation events closely follows a similar increase in 2-m air temperature (not shown), likely reflecting frontal passages associated with extratropical storms. However, since soil temperature is near or above freezing for these events, the variations in soil temperature likely do not contribute to the excess streamflow.

f. Antecedent conditions

Although it is common to have heavy or extreme precipitation events just before HSFEs, it is not clear whether precipitation in general is higher than normal for an extended period of time before HSFEs (leading to increased frequency of HSFEs during particularly wet winters or springs). To determine this, we look at a 14-day ''antecedent'' period preceding our estimates of WRT (2–5 days for Charles gauge, and 0–1 day for the Mystic gauge). The antecedent period is close enough to HSFEs to potentially influence streamflow, but outside of the confounding effects of rainfall within the WRT. Hence, for the Charles (Mystic) gauge, we examine precipitation from days 19 to 6 (15 to 2) before each HSFE peak to determine if total precipitation during this period is higher or lower than normal. To define ''normal'' conditions, we calculate the total precipitation that occurs in the preceding 14-day window, offset by the WRT, for each gauge and each day 1950–2014, excluding the first 16 (19) days of the record for the Mystic (Charles). Therefore, for each day, there is an associated 14-day antecedent value. The values are converted to anomalies by subtracting the long-term daily means of these values (see section 2d). Each daily anomaly is converted to a standardized anomaly by subtracting the mean and dividing by the standard deviation of all daily anomaly values, resulting in a standardized anomalous antecedent precipitation value corresponding to each day in the record. The dataset is then randomly

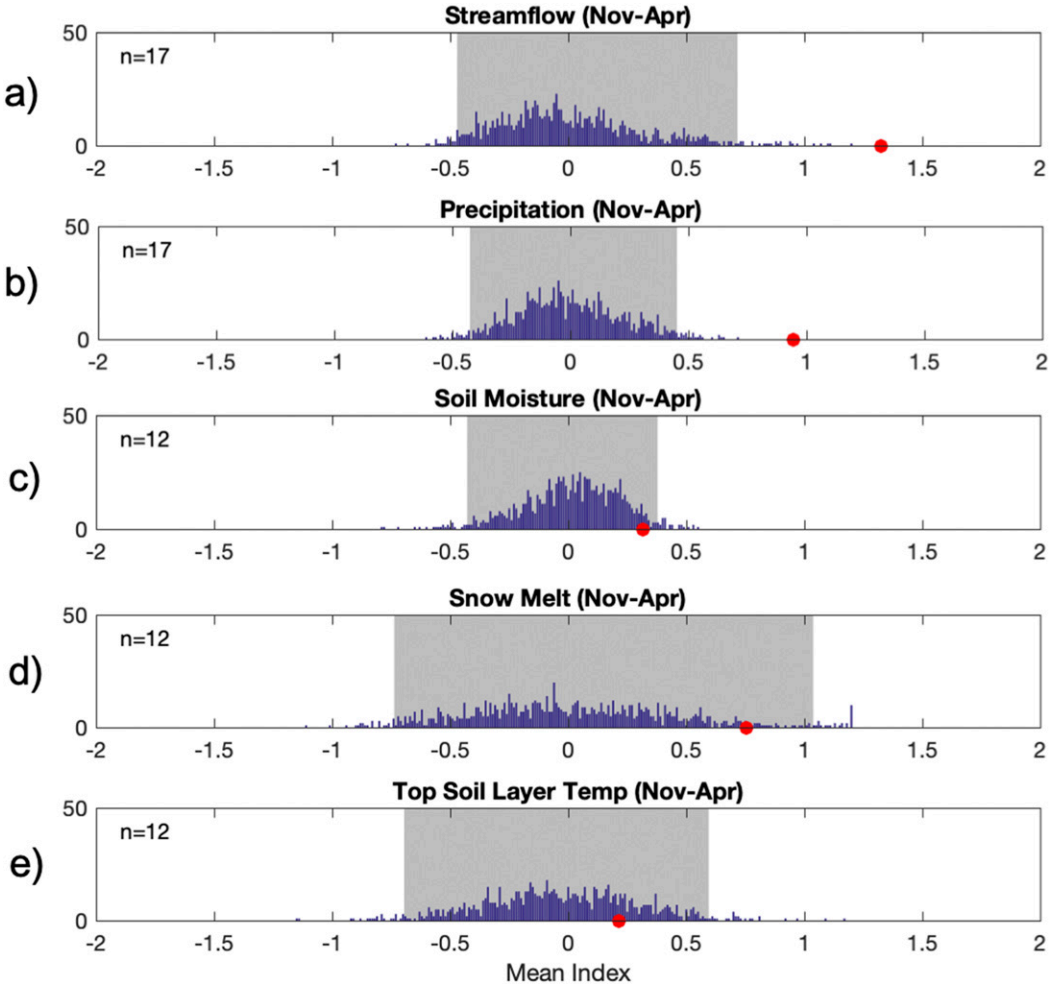

FIG. 7. Mystic basin mean antecedent index (red dots) of 1950–2014 November–April HSFEs for (a) streamflow and (b) precipitation, and of 1980–2008 November–April HSFEs for (c) soil moisture, (d) snowmelt, and (e) top soil layer temperature. The number of HSFEs considered is shown in the top left of each panel. The antecedent index for any HSFE is the 14-day mean value (beginning 16 days before and ending 2 days before the HSFE peak), reduced to a standardized anomaly of all possible 14-day mean values for the November–April period. The blue bars represent a histogram of mean antecedent indices for 1000 randomly selected November–April samples (with sample size as indicated for each panel), and the gray shading denotes the 95% confidence interval of the histogram values.

sampled, preserving both the number and seasonality of the HSFEs, and the mean standardized anomalous antecedent precipitation is calculated for the random sample. This is done 1000 times and the 95th percentile confidence interval of the mean standardized anomalous antecedent precipitation is determined. The actual standardized anomalous antecedent precipitation for the HSFEs is compared to this range, and values outside the confidence interval are considered significantly higher or lower than normal (at the 0.05 level). This technique is similarly applied to streamflow, as well as MERRA-Land soil moisture, snowmelt, and top layer soil temperature, although the analysis for the MERRA-Land variables is limited to 1980–2014. Because snow and soil temperature are important factors only for winter events, the events are divided into cold season (November–April) and warm season (May–October) events. Table 2 summarizes the results, while Figs. 7 and 8 show histograms of the November–April results.

For both basins, streamflow and precipitation are all significantly higher (at the 0.05 level) in the antecedent period preceding HSFEs during the cold season. For the Mystic, soil moisture and snowmelt preceding cold season HSFEs are very high, but within the bounds of normal; whereas for the Charles, soil moisture and

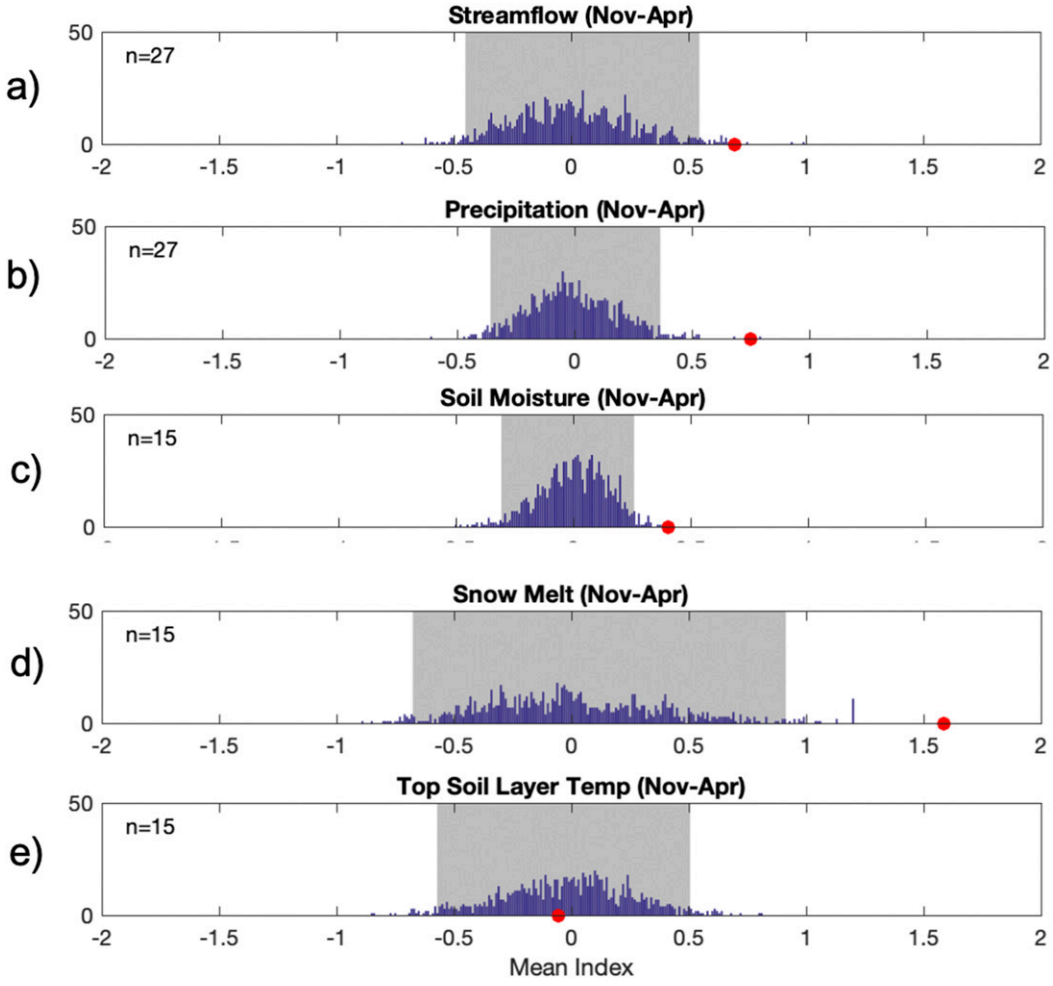

FIG. 8. As in Fig. 7, but for the Charles basin, beginning 19 days before, and ending 6 days before the HSFE peak.

snowmelt are significantly higher than normal at the 0.05 level. Antecedent soil temperature is not outside the range of normal for HSFEs for either gauge. This suggests that for the Charles, antecedent snowmelt may play a role in increasing soil moisture, and both high levels of antecedent soil moisture and precipitation may be necessary to produce cold season HSFEs. For the Mystic, these results suggest that HSFEs tend to occur during particularly ''wet periods,'' with or without accompanying snowmelt, or other confounding factors.

For the warm season, antecedent precipitation is significantly higher than normal for both basins, but antecedent streamflow and soil moisture are not higher than normal. This highlights how extreme precipitation is likely necessary to produce HSFEs during a time of year when antecedent soil moisture does not favor flooding—illustrating why the warm season in the Northeast is typically a flood-poor time of year (Collins 2019). Four of the six August–October Mystic HSFEs (and one of the two Charles HSFEs) examined here were preceded by extreme precipitation events that occur within 500 km of a tropical cyclone, storm, or depression. Although the majority of late-summer extreme precipitation in the Northeast is not related to tropical systems (Huang et al. 2018; Agel et al. 2015), there may be a link between the warm season HSFEs such as those examined here, and precipitation linked to tropical systems.

g. Relationship to extratropical cyclones

In the previous section, we examined which surface hydrological factors play a role in the lead-up to HSFEs. In this section, we look at the links between these antecedent conditions and large-scale meteorological features, such as extratropical cyclones. Although smaller-scale factors (mesoscale and microscale) are not directly considered here, these factors are often embedded within circulation characteristics at a larger scale. Since extreme precipitation is linked to HSFEs, we look at

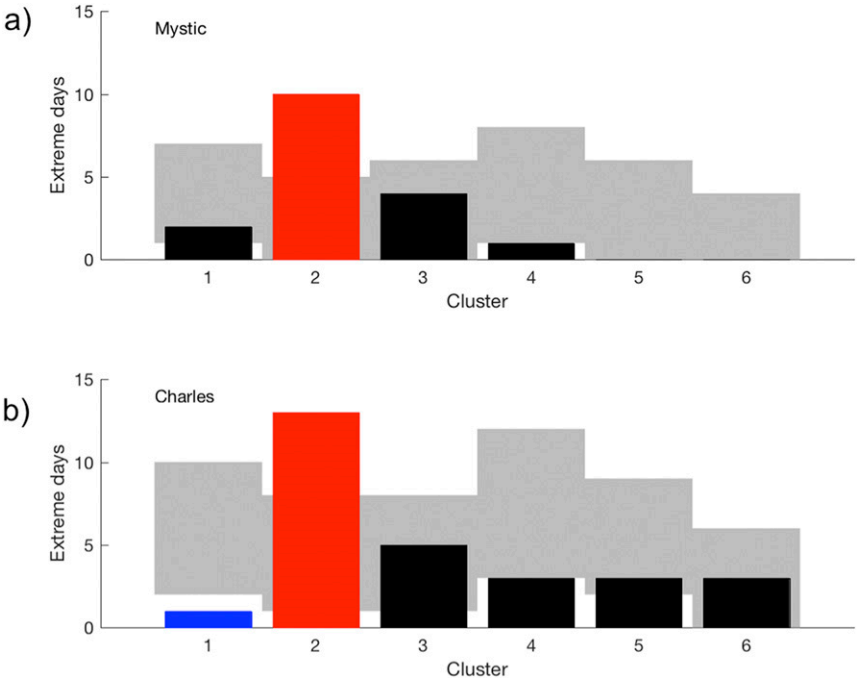

FIG. 9. The number of top 1% Northeast precipitation days occurring 0–1 days before peak streamflow of HSFEs for the (a) Mystic and 2–5 days before peak streamflow of HSFEs for the (b) Charles, separated into six bins. Each bin represents a previously recognized large-scale circulation pattern (group of days with similar characteristics, labeled C1–C6) of tropopause height associated with extreme Northeast precipitation (Agel et al. 2018). Bars are red (blue) if the value is significantly larger (smaller) than that obtained through random resampling. The 95% confidence intervals based on random resampling are shown as gray bars. The top 1% Northeast daily precipitation is based on USHCN daily station data, 1979–2008, as in Agel et al. (2015).

large-scale meteorological patterns (LSMPs; Grotjahn et al. 2016) on extreme precipitation days.

From Agel et al. (2018), extreme precipitation (top 1% daily precipitation 1979–2008) in the Northeast is linked to six large-scale meteorological patterns of troposphere height (Fig. S1 in the online supplemental material, with each pattern labeled C1 through C6). Troposphere height patterns (troughs and ridges) are linked to jet stream structures and upper-level steering mechanisms of synoptic systems (Bosart 1999; Hoskins et al. 1985). For the Mystic gauge, 14 HSFEs occur from 1980 to 2008. For these events, a total of 17 extreme precipitation days occur in a 1-day window preceding the peaks (the WRT for this gauge). Each of these extreme precipitation days is represented by one of the troposphere height patterns, the distribution of which is shown in Fig. 9. The majority of extreme days associated with HSFEs are linked to the C2 pattern. Similarly, for the Charles gauge 17 HSFEs occur 1980–2008, and 28 extreme precipitation days occur in the 2–5-day window preceding the peaks (the WRT for this gauge), of which the majority of the extreme precipitation days are assigned to the C2 pattern. This pattern is linked to strong coastal storms occurring predominantly in late winter and early spring (Agel et al. 2018). These storms generally feature intense low pressure centers that track northward from offshore New Jersey toward Maine, feeding moisture from the western Atlantic into extreme eastern New England. These results support the conclusions of Collins et al. (2014), who found that coastal lows were associated with higher magnitude annual floods in New England and Atlantic Canada rivers.

Because of the dominance of the C2 large-scale meteorological pattern with respect to Mystic and Charles HSFEs, we examine several aspects of these pattern days. In Figs. 10 and 11, MSLP, precipitation, IVT, soil moisture, and snowmelt are composited for the Mystic and Charles C2 extreme days, respectively, that occur within the WRT for the HSFEs, 1980–2008. The MSLP patterns show strong coastal surface lows along the southern New England coastline, with slightly deeper lows for the Charles. Heavy precipitation is evident along the coastal regions, and IVT is particularly strong for eastern Massachusetts. The soil moisture is anomalously

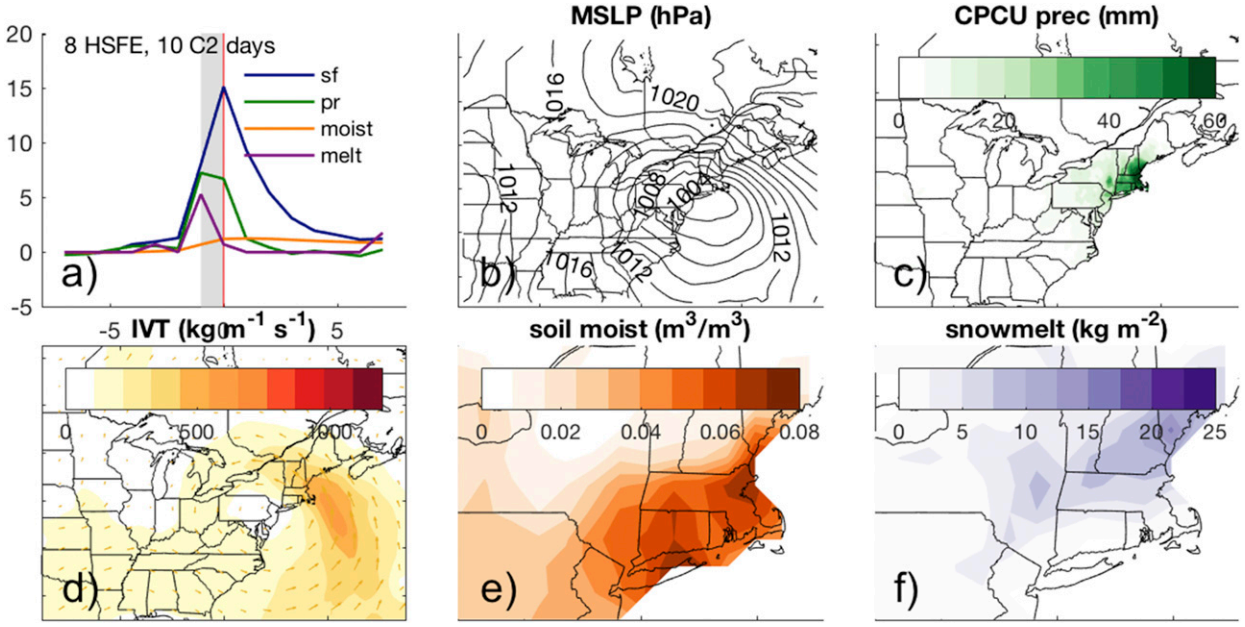

FIG. 10. Composites of (a) ±7-day trace of standardized streamflow, precipitation, moisture, and snowmelt centered on the day of peak streamflow (vertical red line) for 1980–2008 HSFEs that feature C2 coastal storms (Agel et al. 2018) that occur 0–1 day (gray shading) before the HSFE peak for the Mystic basin. The number of composited events and extreme precipitation days are shown at top left. Also shown are composites of (b) mean sea level pressure, (c) precipitation, (d) integrated moisture transport, (e) soil moisture, and (f) snowmelt for the HSFE days featuring C2 storms.

high along the basins of interest, in agreement with the days preceding the HSFEs in Figs. 4e,f and 5e,f. Snowmelt is also anomalously high along the basins of interest (despite including low-snow C2 days occurring May–October). Consistent with our other findings, precipitation during C2 HSFE events for the Mystic is more intense than that for the Charles, while IVT associated with Charles C2 events shows a deeper moisture source

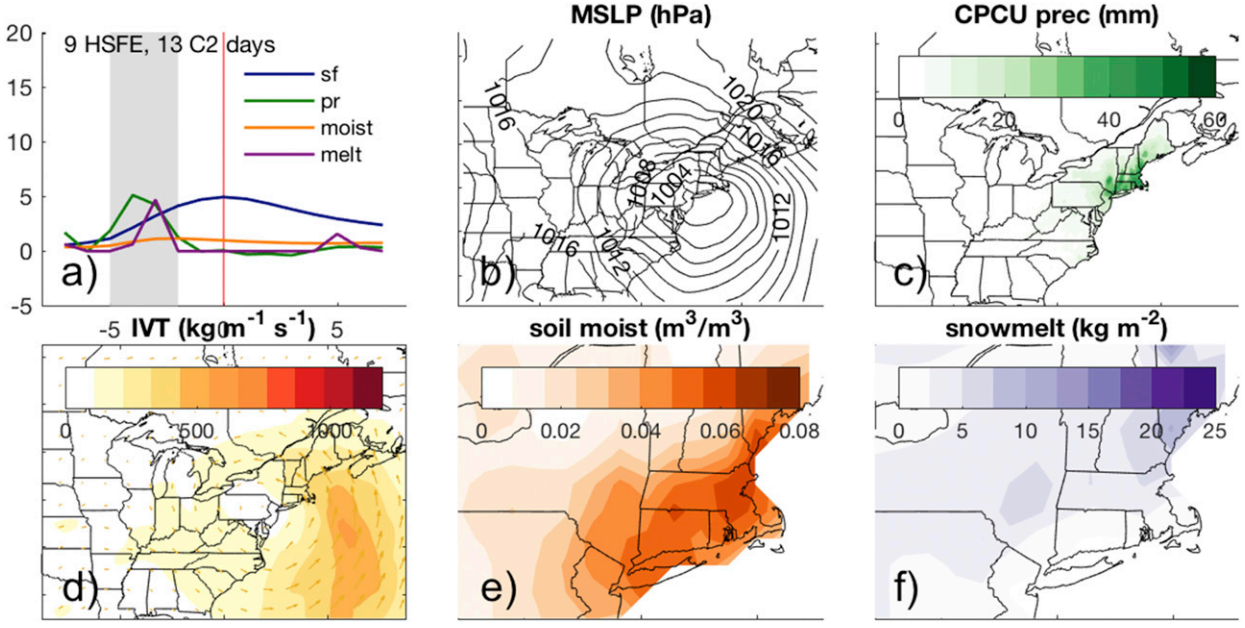

FIG. 11. As in Fig. 10, but for the 1980–2008 HSFEs that feature C2 coastal storms (Agel et al. 2018) that occur 2–5 days before the HSFE peak for the Charles basin.

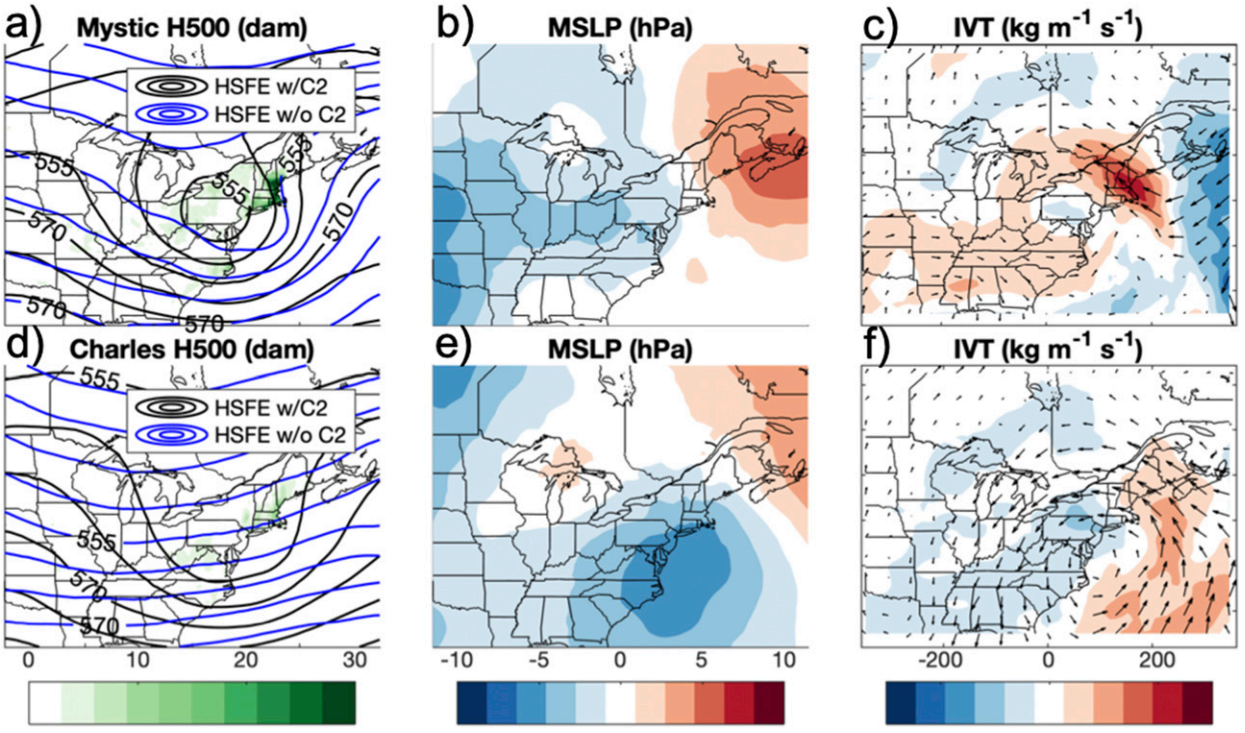

FIG. 12. Differences between composites of Mystic HSFEs 1980–2008 (top) that feature C2 LSMP days (Agel et al. 2018) that occur 0–1 day before peaks in HSFEs and those that do not feature C2 days for (a) MERRA-2 500-hPa geopotential height contours (days followed by HSFEs shown as black lines, days not followed by HSFEs shown as blue lines) and CPCU precipitation (mm; shaded), (b) MERRA-2 MSLP, and (c) MERRA-2 IVT. (d)–(f) As in (a)–(c), but for the Charles basin, except for differences in composites of HSFEs that feature C2 days that occur 2–5 days before peaks in HSFEs and those that do not feature C2 days.

extending to the warm waters to the east of Florida, providing the potential for longer-duration precipitation events for the Charles.

In Fig. 12, the differences in 500-hPa geopotential height, precipitation, MSLP anomalies, and IVT anomalies between HSFEs that feature C2 days and those that do not are evaluated for each basin. For the Mystic, the upper-level circulation is more closed, and IVT and precipitation are more intense on HSFE days featuring C2 days. For the Charles, the coastal low location and intensity are more pronounced on C2 days, and the IVT anomalies, although not as pronounced as for the Mystic, extend farther into the warm waters off Florida.

In Fig. 13, the differences in precipitation duration, precipitation intensity, and total precipitation for HSFEs that feature C2 days and those that do not are shown. For the Mystic, C2 HFSEs have higher intensity, and therefore higher total precipitation than for non-C2 HSFEs. For the Charles, C2 HSFEs have both slightly longer duration and slightly higher intensity than for non-C2 HSFEs, leading to higher total precipitation for C2 HSFEs.

Finally, when all days 1980–2008 with circulation patterns similar to C2 are considered (Fig. 14), those that are closely followed by HSFEs in the Mystic basin tend to feature more precipitation, slightly stronger coastal storms, and stronger IVT directed at southern New England; while those that are followed closely by HSFEs in the Charles basin tend to feature more precipitation, a deeper Mid-Atlantic coastal low, and more IVT directed into eastern Massachusetts. Upper-level circulation tends to be closed for all C2 days, regardless of whether or not they are followed by HSFEs. While the strongest IVT differences occur directly over coastal Massachusetts for the Mystic, for the Charles the maximum IVT differences occur to the south of the region. However, the extended IVT flow in conjunction with the closed upper-level flow shows potential for longer-duration precipitation for the Charles basin.

4. Summary and discussion

In this study, we examine high streamflow events (HSFEs), defined as continuous days of streamflow above the mean annual maxima, 1950–2014, within the Charles and Mystic basins of eastern Massachusetts, in relation to various meteorological factors. Key findings include the following:

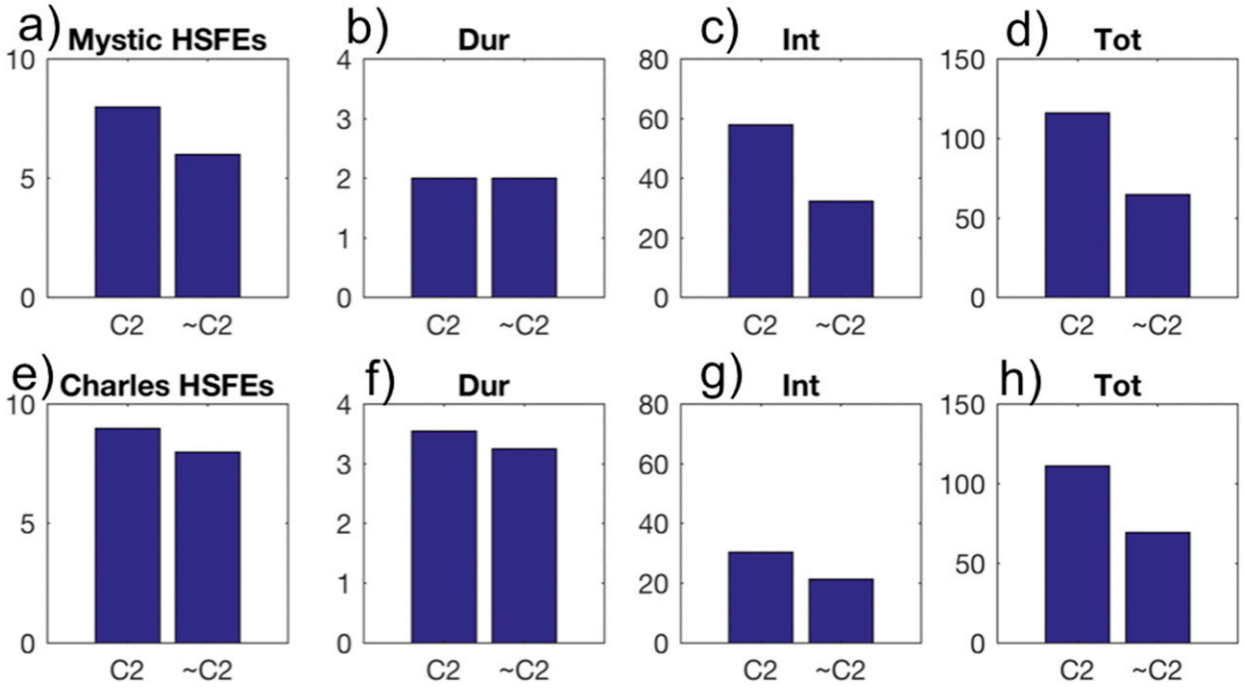

FIG. 13. For Mystic HSFEs (1980–2008) that feature C2 LSMP days (Agel et al. 2018) that occur 0–1 day before peaks in HSFEs (labeled C2) and those that do not feature C2 days (labeled ~C2), shown are the (a) number of events, (b) mean precipitation duration (days), (c) mean intensity of precipitation (mm day^{-1}), and (d) mean precipitation total (mm) for the 2-day window representing the basin WRT. (e)–(h) As in (a)–(d), but for the Charles, except for the 4-day window that occurs 2–5 days before HSFE peak streamflow.

- For both basins, the majority of HSFEs (~52% for the Mystic; ~80% for the Charles) occur from late winter through early summer (February–June).
- For the Charles basin, HSFEs typically last for 3–9 days (73.5%), while for the Mystic basin, 48.1% occur on a single day, and ~90% last for 1–3 days.
- Extreme or heavy precipitation tends to precede HSFEs (90% of events for the Mystic and nearly 45% for the Charles), and this precipitation peaks on average 2–5 days before HSFE peaks for the Charles, and 0–1 day before HSFE peaks for the Mystic, consistent with the watershed response times of the respective basins.
- Less than 30% of extreme precipitation events are followed by HSFEs in the Mystic, while only 20% of extreme precipitation events are followed by HSFEs in the Charles, reflecting the relatively low flashiness of the basins, and the relative importance of other factors in generating HSFEs.
- For cold season HSFEs in the Charles basin, antecedent streamflow, precipitation, soil moisture, and snowmelt are all statistically higher than average in the 2-week period before the incipient precipitation events, suggesting that HSFEs occur more often when the conditions are ''primed'' for maximum streamflow (i.e., when the basin has no more capacity to ''store'' additional water input). For cold season HSFEs in the Mystic basin, only antecedent streamflow and precipitation are statistically higher than average in the 2-week period prior to the incipient precipitation events (soil moisture is high but not significantly so), suggesting that HSFEs are tied more strongly to precipitation than to other factors such as storage in this basin. For warm season HSFEs, antecedent precipitation is statistically higher than average in the period prior to the main preceding (often extreme) precipitation event.
- More than half of the HSFEs in both basins are preceded by at least one extreme precipitation day associated with a large-scale meteorological pattern identified as the C2 pattern in Agel et al. (2018). This pattern is consistent with strong spring coastal storms, in which areas of low pressure form off the Atlantic coastline and move northeastward toward New England, transporting large streams of ocean-fed moisture ahead of the storm itself. The more intense the surface low and/or the greater the moisture feed, the more likely a C2-pattern storm is associated with a HSFE.

An important feature of this study is the examination of what meteorological conditions or variations in synoptic storms may be associated with HSFEs in one adjacent basin and not the other, potentially assisting

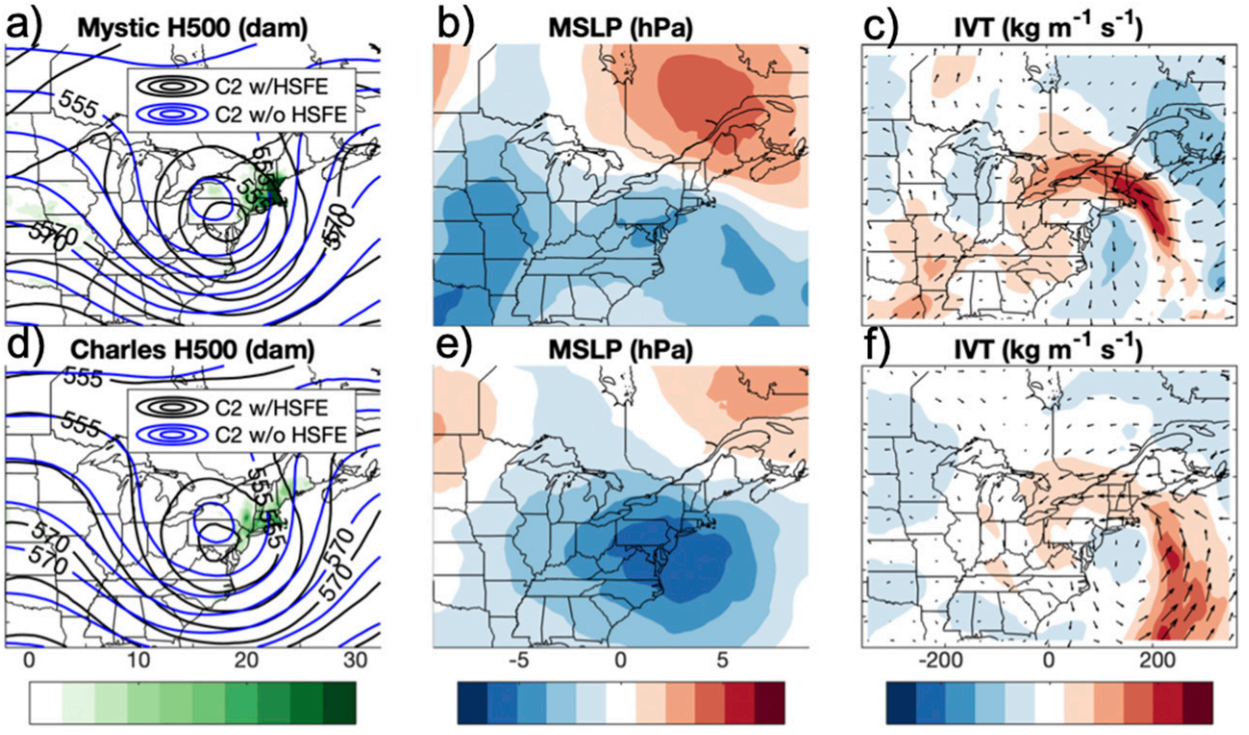

FIG. 14. As in Fig. 12, but for the differences in composites of all C2 days, 1980–2008, that directly precede HSFEs, and C2 days that do not precede HSFEs within their WRT, for the (a)–(c) Mystic and (d)–(f) Charles.

flood forecasting for this region. In this case, due to the comparatively high flashiness of the Mystic basin, single pulses of short-duration, high-intensity precipitation often precede HSFEs, whereas for the Charles, longer-duration precipitation events possibly containing multiple days of extreme precipitation often precede HSFEs. Although both basins' HSFEs are linked frequently to C2-pattern storms (i.e., nor'easters), it is important to distinguish between storms that deliver concentrated intense precipitation to the immediate Boston area (affecting the Mystic) and those that result in more widespread, longer-duration precipitation, or are embedded in unusually wet periods, or periods of intense snowmelt (affecting the Charles).

The passage of synoptic storms associated with the extreme precipitation that tends to occur before HSFEs can also provide insight into the behavior of snowmelt and surface temperature surrounding HSFEs. As extratropical storms often include leading warm fronts, some of the snowmelt (and decreasing snow mass) that occurs just before HSFEs is likely associated with increasing near-surface temperatures. The system's trailing cold front may then induce precipitation in the form of snow, leading to increases in snow mass and snowmelt during and after the onset of the preceding precipitation event, as seen in Figs. 5 and 6.

The key takeaway for this study is that for the Metro Boston area, although extreme precipitation is often a necessary ingredient in generating HSFEs, most HSFEs also occur in the presence of other factors. The majority of HSFEs for these two basins, particularly during the winter and spring, can be attributed to 1) seasonally high precipitation due to coastal storms, particularly nor'easters, 2) seasonally high soil moisture, and 3) high antecedent streamflow. However, other factors not examined here may also influence the frequency of occurrence and intensity of HSFEs, including time of leaf-on and leaf-off (which affects evapotranspiration rates, and thus antecedent soil moisture and streamflow conditions), the role of rain-on-snow events, and water retention and runoff. The study of these additional factors is left to future work.

Acknowledgments. The work of L. Agel and M. Barlow is funded by National Science Foundation Project AGS 1623912. This work was also funded in part by a Commonwealth of Massachusetts Supplemental Environmental Bond Bill supported by Senator William N. Brownsberger. The scientific results and conclusions, as well as any views or opinions

expressed herein, are those of the author(s) and do not necessarily reflect those of NOAA or the Department of Commerce.

REFERENCES

Agel, L., M. Barlow, J.-H. Qian, F. Colby, E. Douglas, and T. Eichler, 2015: Climatology of daily precipitation and extreme precipitation events in the northeast United States. *J. Hydrometeor.*, **16**, 2537–2557, https://doi.org/10.1175/JHM-D-14-0147.1.

——, ——, S. B. Feldstein, and W J. Gutowski Jr., 2018: Identification of large-scale meteorological patterns associated with extreme precipitation in the US northeast. *Climate Dyn.*, **50**, 1819–1839, https://doi.org/10.1007/s00382-017-3724-8.

——, ——, F. Colby, H. Binder, J. L. Catto, A. Hoell, and J. Cohen, 2019: Dynamical analysis of extreme precipitation in the US northeast based on large-scale meteorological patterns. *Climate Dyn.*, **52**, 1739–1760, https://doi.org/10.1007/s00382-018-4223-2.

Armstrong, W. H., M. J. Collins, and N. P. Snyder, 2012: Increased frequency of low-magnitude floods in New England. *J. Amer. Water Resour. Assoc.*, **48**, 306–320, https://doi.org/10.1111/j.1752-1688.2011.00613.x.

——, ——, and ——, 2014: Hydroclimatic flood trends in the northeastern United States and linkages with large-scale atmospheric circulation patterns. *Hydrol. Sci. J.*, **59**, 1636–1655, https://doi.org/10.1080/02626667.2013.862339.

Ashley, S. T., and W. S. Ashley, 2008: Flood fatalities in the United States. *J. Appl. Meteor. Climatol.*, **47**, 805–818, https://doi.org/10.1175/2007JAMC1611.1.

Baker, D. B., R. P. Richards, T. T. Loftus, and J. W. Kramer, 2004: A new flashiness index: Characteristics and applications to midwestern rivers and streams. *J. Amer. Water Resour. Assoc.*, **40**, 503–522, https://doi.org/10.1111/j.1752-1688.2004.tb01046.x.

Bosart, L. F., 1999: Observed cyclone life cycles. *The Life Cycles of Extratropical Cyclones*, M. A. Shapiro and S. Grønås, Eds., Amer. Meteor. Soc., 187–213.

Chen, M., P. Xie, and CPC Precipitation Working Group, 2008: CPC Unified gauge-based analysis of global daily precipitation. *2008 Western Pacific Geophysics Meeting*, Cairns, Australia, Amer. Geophys. Union, ftp://ftp.cpc.ncep.noaa.gov/precip/CPC_UNI_PRCP/GAUGE_CONUS/DOCU/Chen_et_al_2008_Daily_Gauge_Anal.pdf.

Collins, M. J., 2009: Evidence for changing flood risk in New England since the late 20th century. *J. Amer. Water Resour. Assoc.*, **45**, 279–290, https://doi.org/10.1111/j.1752-1688.2008.00277.x.

——, 2019: River flood seasonality in the Northeast United States: Characterization and trends. *Hydrol. Processes*, **33**, 687–698, https://doi.org/10.1002/hyp.13355.

——, and Coauthors, 2014: Annual floods in New England (USA) and Atlantic Canada: Synoptic climatology and generating mechanisms. *Phys. Geogr.*, **35**, 195–219, https://doi.org/10.1080/02723646.2014.888510.

Dingman, S. L., 2002: *Physical Hydrology*. 2nd ed. Prentice Hall, 646 pp.

Easterling, D. R., T. R. Karl, J. H. Lawrimore, and S. A. Del Greco, 1999: United States Historical Climatology Network daily temperature, precipitation, and snow data for 1871–1997. ORNL/CDIAC-188, NDP-070, Carbon Dioxide Information Analysis Center, 94 pp.

Federal Emergency Management Agency, 2006: Mass. Disaster aid surpasses $70 million for May floods. http://www.fema.gov/news-release/2006/09/22/mass-disaster-aid-surpasses-70-million-may-floods.

Frei, A., K. E. Kunkel, and A. Matonse, 2015: The seasonal nature of extreme hydrological events in the northeastern United States. *J. Hydrometeor.*, **16**, 2065–2085, https://doi.org/10.1175/JHM-D-14-0237.1.

Gelaro, R., and Coauthors, 2017: The Modern-Era Retrospective Analysis for Research and Applications, version 2 (MERRA-2). *J. Climate*, **30**, 5419–5454, https://doi.org/10.1175/JCLI-D-16-0758.1.

Graybeal, D. Y., and D. J. Leathers, 2006: Snowmelt-related flood risk in Appalachia: First estimates from a historical snow climatology. *J. Appl. Meteor. Climatol.*, **45**, 178–193, https://doi.org/10.1175/JAM2330.1.

Grotjahn, R., and Coauthors, 2016: North American extreme temperature events and related large scale meteorological patterns: A review of statistical methods, dynamics, modeling, and trends. *Climate Dyn.*, **46**, 1151–1184, https://doi.org/10.1007/s00382-015-2638-6.

Hawcroft, M. K., L. C. Shaffrey, K. I. Hodges, and H. F. Dacre, 2012: How much Northern Hemisphere precipitation is associated with extratropical cyclones? *Geophys. Res. Lett.*, **39**, L24809, https://doi.org/10.1029/2012GL053866.

Hoskins, B. J., M. E. McIntyre, and A. W. Robertson, 1985: On the use and significance of isentropic potential vorticity maps. *Quart. J. Roy. Meteor. Soc.*, **111**, 877–946, https://doi.org/10.1002/qj.49711147002.

Huang, H., J. M. Winter, E. C. Osterberg, R. M. Horton, and B. Beckage, 2017: Total and extreme precipitation changes over the northeastern United States. *J. Hydrometeor.*, **18**, 1783–1798, https://doi.org/10.1175/JHM-D-16-0195.1.

——, ——, and ——, 2018: Mechanisms of abrupt extreme precipitation change over the northeastern United States. *J. Geophys. Res. Atmos.*, **123**, 7179–7192, https://doi.org/10.1029/2017JD028136.

Ivancic, T. J., and S. B. Shaw, 2015: Examining why trends in very heavy precipitation should not be mistaken for trends in very high river discharge. *Climatic Change*, **133**, 681–693, https://doi.org/10.1007/s10584-015-1476-1.

Kunkel, K., and Coauthors, 2013: Regional climate trends and scenarios for the U.S. National Climate Assessment: Part 1—Climate of the Northeast U.S., NOAA Tech. Rep. NESDIS 142-1, 80 pp., https://www.nesdis.noaa.gov/sites/default/files/asset/document/NOAA_NESDIS_Tech_Report_142-1-Climate_of_the_Northeast_US.pdf.

Landsea, C. W., and J. L. Franklin, 2013: Atlantic hurricane database uncertainty and presentation of a new database format. *Mon. Wea. Rev.*, **141**, 3576–3592, https://doi.org/10.1175/MWR-D-12-00254.1.

Melillo, J. M., T. C. Richmond, and G. W. Yohe, Eds., 2014: *Climate Change Impacts in the United States: The Third National Climate Assessment*. U.S. Global Change Research Program, 841 pp., https://doi.org/10.7930/J0Z31WJ2.

Peterson, T. C., P. A. Stott, and S. Herring, 2012: Explaining Extreme Events of 2011 from a Climate Perspective. *Bull. Amer. Meteor. Soc.*, **93** (7), 1041–1067, https://doi.org/10.1175/BAMS-D-12-00021.1.

Pfahl, S., and H. Wernli, 2012: Quantifying the relevance of cyclones for precipitation extremes. *J. Climate*, **25**, 6770–6780, https://doi.org/10.1175/JCLI-D-11-00705.1.

Reichle, R. H., R. D. Koster, G. J. M. De Lannoy, B. A. Forman, Q. Liu, S. P. P. Mahanama, and A. Touré, 2011: Assessment and enhancement of MERRA land surface hydrology estimates. *J. Climate*, **24**, 6322–6338, https://doi.org/10.1175/JCLI-D-10-05033.1.

Slater, L. J., and G. Villarini, 2016: Recent trends in U.S. flood risk. *Geophys. Res. Lett.*, **43**, 12 428–12 436, https://doi.org/10.1002/2016GL071199.

Towey, K. L., J. F. Booth, A. Frei, and M. R. Sinclair, 2018: Track and circulation analysis of tropical and extratropical cyclones that cause strong precipitation and streamflow events in the New York City watershed. *J. Hydrometeor.*, **19**, 1027–1042, https://doi.org/10.1175/JHM-D-17-0199.1.

Wolman, M. G., and J. P. Miller, 1960: Magnitude and frequency of forces in geomorphic processes. *J. Geol.*, **68**, 54–74, https://doi.org/10.1086/626637.